JOURNAL OF MATERIALS SCIENCE 27 (1992) 869–875

Role of phosphorus content on porosity of cast irons

T. S. SUDARSHAN
Materials Modification Inc, PO Box 4817, Falls Church, VA 22044, USA
T. S. SRIVATSAN
Department of Mechanical Engineering, The University of Akron, Akron, OH 44325-3903, USA

The influence of phosphorus content on two cast-iron cylinder liner specimens containing different levels of phosphorus has been studied using analytical techniques. X-ray photoelectron spectroscopy and energy dispersive X-ray analysis were used to relate the surface roughness of a cast-iron specimen with phosphorus content. The sample with higher phosphorus content had higher levels of porosity. The increased porosity is ascribed to the formation of the phosphide eutectic. Scanning electron microscopy observations were also used to relate the phosphorus content in the sample with amount and size of microporosity. The beneficial influence of phosphorus as an alloying element is highlighted and the detrimental effects arising from the formation of microporosity are discussed.

1. Introduction

Internal combustion (IC) engines may be either water cooled or air cooled, and the cylinder walls of these engines are either integrally cast with the cylinder block or formed from separately cast liners which are inserted in the surrounding water jacket or air-cooled block. For ordinary purposes, where conditions are not particularly arduous, the integrally cast cylinder block is employed, particularly for private transportation vehicles. The material normally chosen is grey cast iron with an approximate composition shown in Table I [1]. Additions of up to 0.3% of chromium are frequently made in order to ensure a fully pearlitic structure in the bore of the cylinder. Such castings have cylinder bore hardnesses ranging from 190 to 225 HB. Additions of small amounts of phosphorus (up to about 0.8%) improves the wear resistance of the grey cast iron [2, 3]. An improvement in wear resistance results in part from an increased hardness of the grey cast iron. Phosphorus, however, has a detrimental effect in that it introduces difficulties during casting.

In commercial applications the liners are centrifugally cast [1–4], and a typical composition is given in Table II. The hardnesses range is typically from 225 to 260 HB and these liners have good resistance to wear. Heat treatments are also used to increase the hardness, resulting in enhanced wear resistance and, consequently, an improvement in life expectancy of the cylinder liner.

The presence of phosphorus in cast iron causes porosity and high levels of phosphorus content should be avoided in order to minimize internal shrinkage and porosity. Internal defects such as porosity adversely affect: (a) the wear resistance, and (b) the pressure tightness of the cylinder liner. Furthermore, from the requirements of soundness, strength and machinability, the use of low phosphorus content is desirable. It is well documented that phosphorus content in excess of 0.2% causes shrinkage porosity in cast iron [5–7]. The shrinkage porosity results from contraction of the phosphorus-rich liquid on cooling from the iron–graphite eutectic temperature to the phosphide eutectic temperature, and by subsequent solidification contraction at the phosphide eutectic temperature [3, 5]. The mechanism of porosity formation suggests that at some temperature above the phosphide eutectic temperature, voids found in the casting are filled with liquid phosphide eutectic. When shrinkage porosity occurs in these cast irons, it is confined to exist at the hot spot of the casting [5].

TABLE I Chemical composition of grey cast iron

Element	Percentage
Total carbon	3.1–3.4
Silicon	1.7–2.2
Manganese	0.6–0.9
Sulphur	0.12 max.
Phosphorus	0.15

TABLE II Chemical composition of the cast-iron cylinder liner

Element	Percentage
Total carbon	3.3–3.5
Silicon	2.2–2.6
Manganese	0.6–1.2
Phosphorus	0.4–0.8
Chromium	Up to 0.5

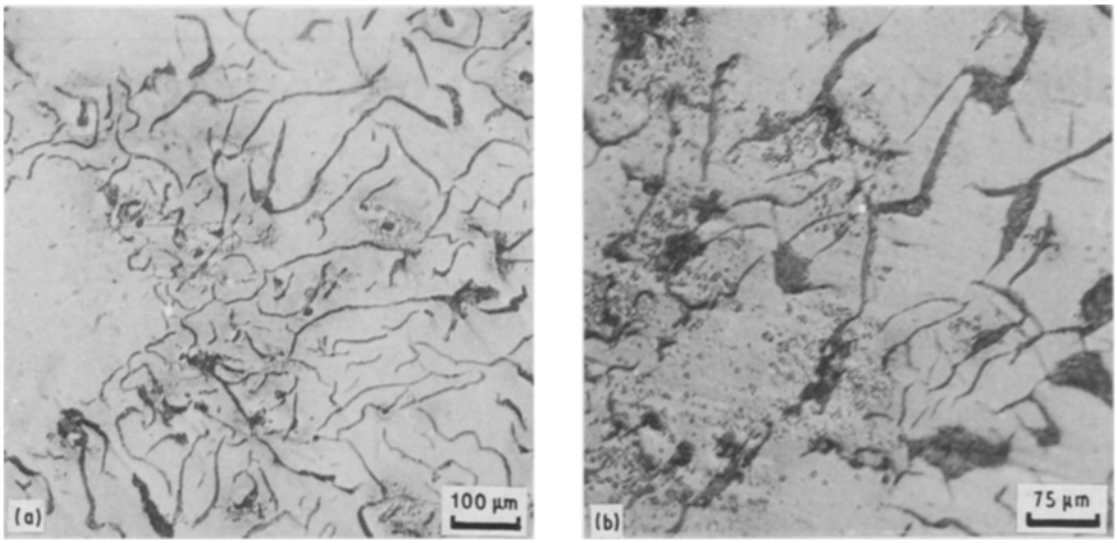

Figure 1 Microstructure of grey cast iron containing phosphorus, showing the presence of phosphide eutectic (a) low phosphorus sample and (b) sample containing high phosphorus.

Unlike other principal alloying elements in grey cast iron, phosphorus forms a complex low melting point eutectic. The low melting point eutectic solidifies at around 200 °C below the iron–carbon–silicon eutectic and segregates to the cell boundaries and hot spots. During cooling, the liquid phosphide eutectic undergoes liquid contraction, and on solidification additional contraction occurs [8, 9]. The contraction of isolated areas of the phosphide eutectic liquid results in unsoundness of the castings. The distribution of phosphide eutectic particles in cast iron containing low and high amounts of phosphorus is shown in Fig. 1.

Hamaker *et al.* [8] reported a correlation between shrinkage porosity and the presence of phosphide eutectic in castings that contained appreciable amounts of phosphorus. They demonstrated that alloying elements chromium and molybdenum increased the amount of phosphide eutectic during solidification, along with an increase in the amount of porosity. The phosphide eutectic is metastable and it solidifies in two forms

(a) an iron–iron phosphide–iron carbide eutectic, and

(b) an iron–iron phosphide–graphite eutectic.

In light sections such as cylinder liners used in automobiles, solidification of the iron–carbon eutectic proceeds inwards from the mould walls and the remaining liquid is enriched in phosphorus content as the low phosphorus iron–carbide eutectic initially solidifies. The remaining hot spot in the centre of the casting contains most of the phosphide eutectic (Fe_3C–Fe_3P) [10, 11]. As a result, the internal liquid upon solidification contracts and produces concentrated voids, referred to as shrinkage porosity that degrades the pressure tightness and adversely affects engine efficiency. Thick cylinder liners such as those used in large industrial engines or marine diesels are thus more susceptible to the detrimental effects of internal porosity.

The purpose of this paper is to examine the effect of phosphorus content on porosity found in two automobile cylinder liners containing different levels of phosphorus.

2. Experimental procedure

The study was carried out on different automobile cylinder liners containing two levels of phosphorus that were produced under identical conditions. The cylinder liners will henceforth be referred to in this paper as samples A and B. Sample A has the liner surface machined to a finish of 150 μm and had a phosphorus content of 0.6%. Sample B had the liner surface machined to a finish of 40 μm and had a phosphorus content of 0.1 to 0.2%.

One test sample was prepared from each cylinder liner for the purpose of X-ray photoelectron spectroscopy (XPS) study. On account of the low phosphorus content in the liners, a fresh fracture surface was created in order to accentuate the phosphorus concentrations. The cast iron was fractured in an atmosphere of inert nitrogen gas. To minimize oxidation and other environmental effects the fractured samples were stored in nitrogen filled test tubes.

Sample A was examined by XPS using a magnesium anode. Initial wide scans were run in order to identify the elements and regions of binding energy. Narrow scan XPS was also performed to study oxidation doublets and shifts of various peaks.

Both samples A and B were also examined by energy dispersive X-ray analysis (EDAX). The fracture surfaces and the liner surfaces of the samples were studied. The EDAX was run on surface pores of the cylinder liner surface and at regions/locations of microporosity on the fracture surface.

The microporosity of the cylinder liners was examined by scanning electron microscopy (SEM). The surfaces of both cylinder liners (samples A and B) were examined at low magnification to identify the number, location and distribution of pores. Examination of the

fracture surface at high magnification was done in order to study microporosity in the fracture surface, and to reveal the morphology of individual pores on the surface.

3. Results and discussion

3.1. X-ray photoelectron spectroscopy

X-ray photoelectron spectroscopy (XPS) was performed on sample A (cylinder liner with surface finish of 150 μm). A wide scan of the sample surface revealed the presence of peaks for the elements iron, carbon and oxygen. The Auger peaks were seen at binding energies of 990 eV for carbon, at 745 eV for oxygen, and three peaks at 550, 610 and 570 eV for iron. The peaks are shown in Fig. 2. A narrow scan was performed on a characteristic peak of each element.

The carbon peak narrow scan was further studied in order to determine the chemical shift and to calibrate the back-scattered energy (BE). The XPS spectra revealed the C1s peak to occur at 962 eV (BE) (Fig. 2). This value accords well with the tabulated value of 964 eV. The carbon peak arises from the presence of carbon in cast iron in the form of iron–carbide (Fe_3C) particles, and also from contamination of the surface with carbon.

The iron doublet was examined with a narrow scan. A peak for $Fe\,2p^3$ was found at 539.5 eV, which accords well with the tabulated value of 540 eV. A peak for Fe_2O_3 was located at 536 eV (Fig. 3). The Fe_2O_3 peak was found to be stronger than the signal for $Fe\ 2p^3$. This is attributed to the oxidation of iron present on the surface. The oxygen doublet was also examined and the O 1s peaks were located at 715 and 717 eV (Fig. 4).

The rationale for performing the XPS study was to

(a) identify the presence and distribution of phosphorus in sample A, and

(b) identify and locate presence of trace elements, such as silicon and chromium.

The XPS study failed, however, to reveal an observable peak for phosphorus or other trace elements present. The absence of an observable peak is attributed to the competing effects of

(i) presence of oxides on the liner surface which suppresses the weaker signals in the spectra data,

(ii) extremely low concentration of these secondary trace elements, which demands multiple scans of the

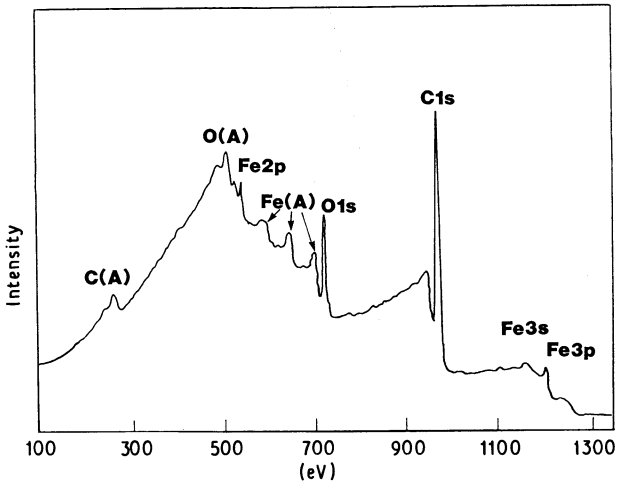

Figure 2 A typical XPS spectrum from sample A (150 μm).

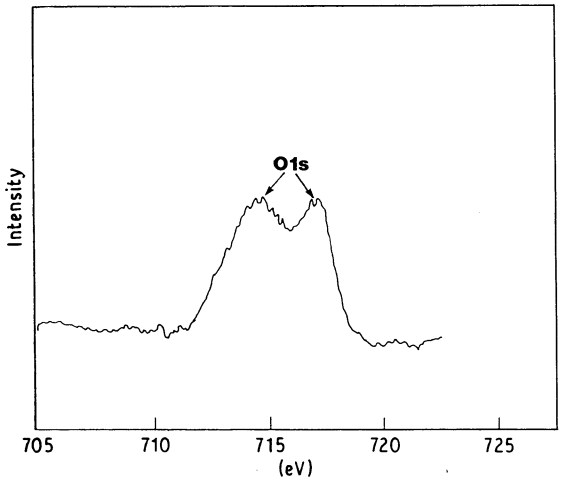

Figure 4 A typical XPS spectrum for identifying oxygen in sample A (150 μm).

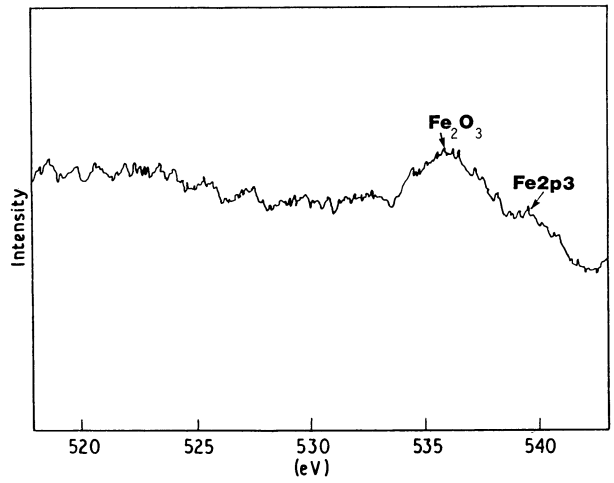

Figure 3 A typical XPS spectrum for identifying the element iron in sample A (150 μm).

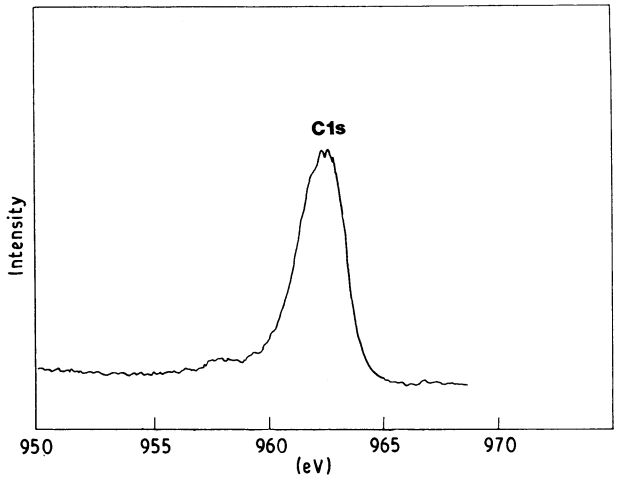

Figure 5 A typical XPS spectrum for identifying carbon in sample A (150 μm).

sample in order to enhance the weak signals given by these low concentration elements, and

(iii) sampling depth which requires that the phosphide eutectic be within 10 nm of the surface.

The XPS study did not provide conclusive information on the amount and/or level of phosphorus contained in the sample.

The roughness of the liner surface in sample A was visible to the naked eye and is attributed to the presence of higher levels of porosity in sample A than the level of porosity present in sample B, which has a smooth liner surface finish (40 μm finish). The increased amount of porosity in sample A, as evident from its rough surface, is due to the presence of higher phosphorus content in the sample.

3.2. Energy dispersive X-ray analysis (EDAX)

EDAX analysis was performed on both samples A and B in an attempt to corroborate with the results and interpretations of the XPS study. Unlike XPS analysis, however, the EDAX study provided some qualitative information on the relative amounts of phosphorus present in the two samples. EDAX of a micropore present on the surface of sample A revealed the presence of phosphorus (Fig. 6a). When the phosphorus peak was amplified by a factor of ten, the presence of trace elements chromium and manganese was detected (Fig. 6b). The presence of chromium facilitates increasing the porosity in cast iron. EDAX of a fine micropore present on the surface of sample B failed to reveal the presence of phosphorus but revealed the presence of silicon (Fig. 7a). Even after amplification of the data by a factor of ten, however, the presence of silicon was detected with no evidence of phosphorus (Fig. 7b). The EDAX study indicates that sample A (150 μm surface finish) had a higher phosphorus content than sample B (40 μm surface finish) and substantiates our interpretations of the data obtained from the XPS study, thus sample A contained higher levels of the phosphide eutectic.

Energy dispersive X-ray analysis was also performed on the fracture surfaces of both samples A and B. In addition to manganese, sulphur was detected on the fracture surface of sample A (Fig. 8a). When amplified by a factor 5, the manganese and sulphur peaks were enlarged, as also the peaks for iron (Fig. 8b). The fracture surface of sample B revealed the presence of iron with no other elements really discernible (Fig. 9a). Amplification of the initial signal by a factor of ten,

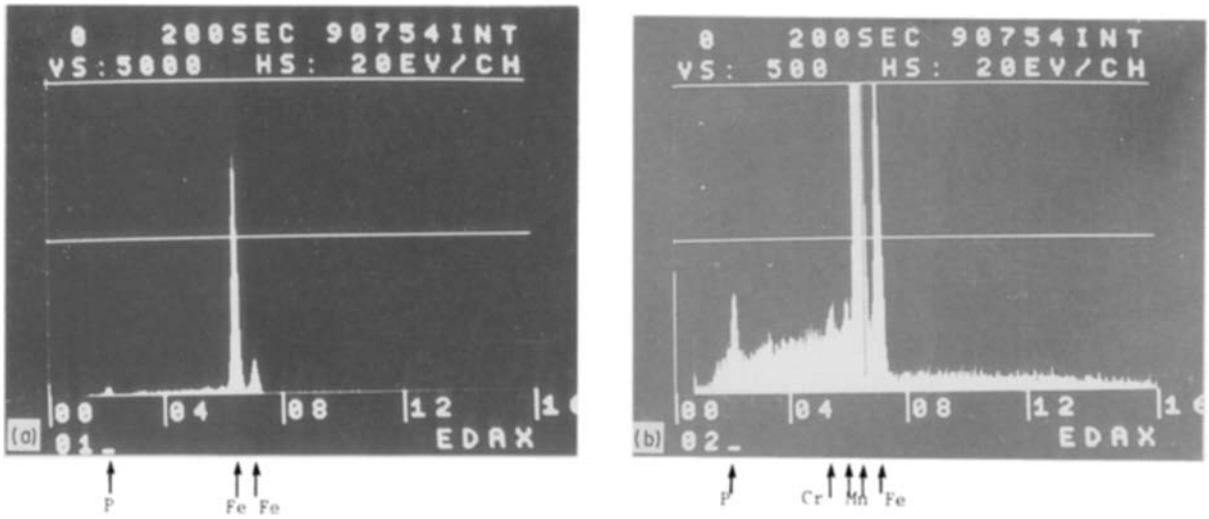

Figure 6 EDAX scan of micropore on sample A showing (a) presence of iron peak and a small peak for phosphorus and (b) enlarged peak for phosphorus and new peaks for chromium and manganese, when amplified by a factor of ten.

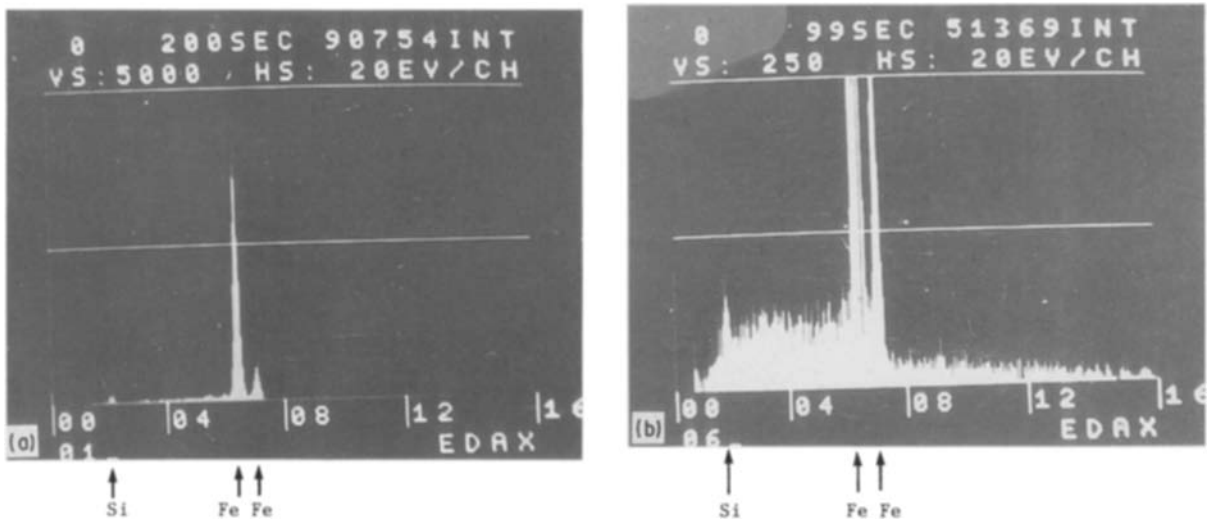

Figure 7 EDAX scan of micropore on surface of sample B showing (a) iron peak and a silicon peak and (b) enlarged peak for silicon with no evidence of phosphorus.

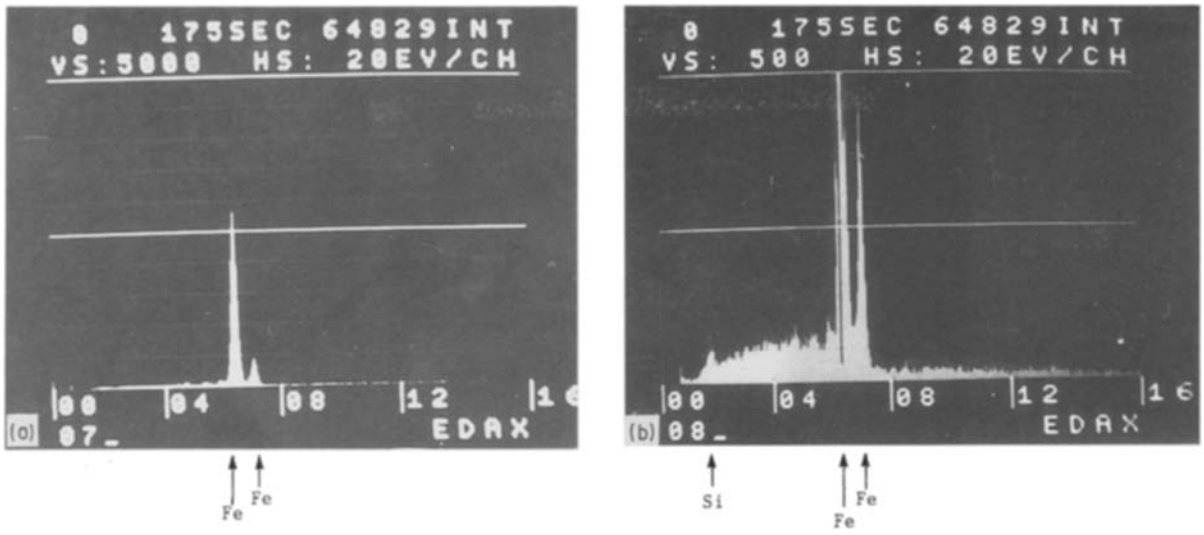

Figure 8 EDAX scan of fracture surface of sample A showing (a) large peaks for iron and a small peak for sulphur and manganese and (b) sulphur and manganese are enlarged when amplified by a factor of five.

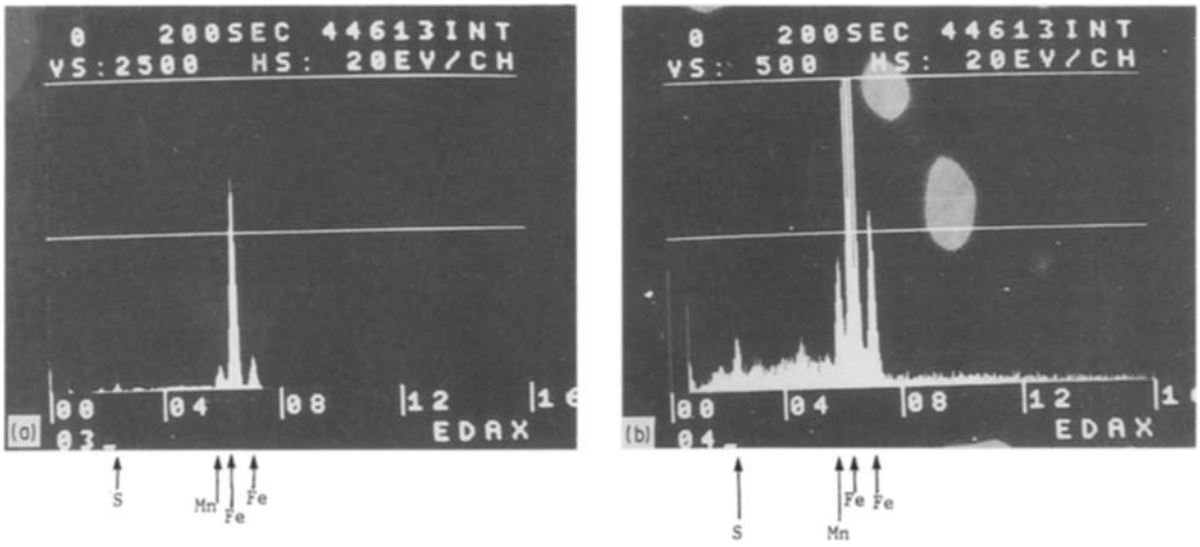

Figure 9 EDAX scan of fracture surface of sample B showing (a) large peaks for iron and (b) evidence of presence of silicon when amplified by a factor of ten.

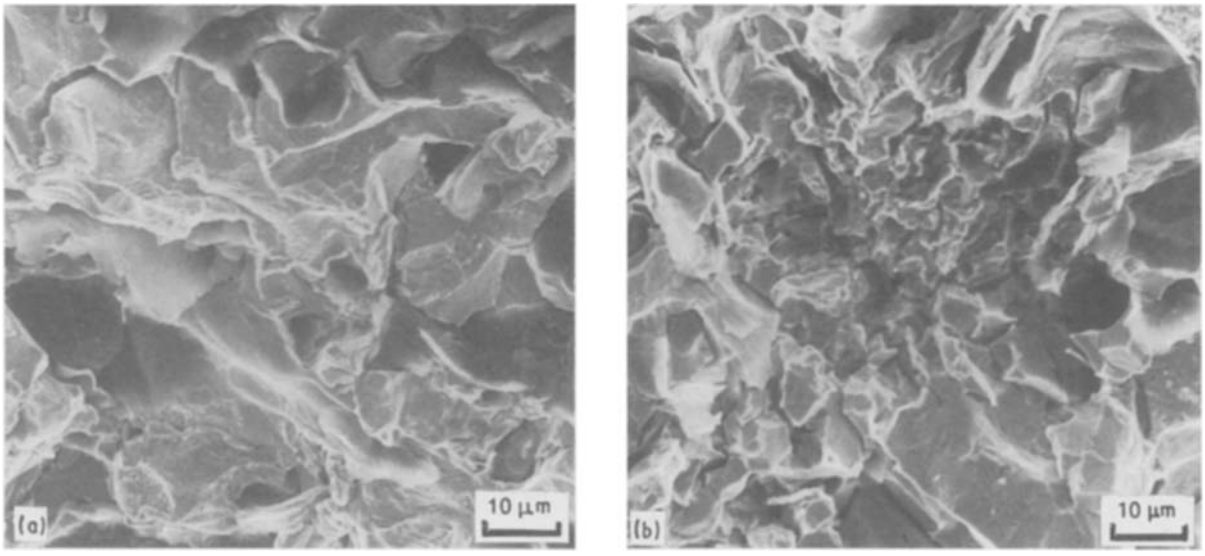

Figure 10 Scanning electron micrograph of the fracture surface of (a) sample B showing few isolated micropores and (b) sample A showing large clusters of microporosity suggesting the presence of high phosphorus content in this sample.

however, revealed the presence of silicon on the fracture surface of the sample (Fig. 9b).

3.3. Scanning electron microscopy

Detailed scanning electron microscopy was performed on both samples in order to elucidate information on the porosity characteristics of each sample. The fracture surfaces of the two samples (samples A and B) revealed entirely different types and amount of porosity. Sample B revealed isolated micropores (Fig. 10a), while sample A revealed large clusters of fine pores (Fig. 10b). The clusters of micropores in sample A were found to be far more numerous than the few isolated pores observed on the fracture surface of sample B.

The clusters of micropores were found to occur at and around regions where the phosphide eutectic had solidified. The phosphide eutectic is the last region to solidify in the cast iron metal, and this results in shrinkage porosity. The amount of phosphide eutectic that forms upon solidification is directly dependent on the amount of phosphorus present in the sample. A higher phosphorus content results in enhanced regions of the phosphide eutectic, and hence, greater shrinkage porosity (Fig. 11).

The inner surfaces of the two samples were also examined by the scanning electron microscope. Sample A revealed a higher density of porosity on the surface than sample B. The large number of surface pores represents areas of shrinkage porosity which were uncovered during machining. The presence of

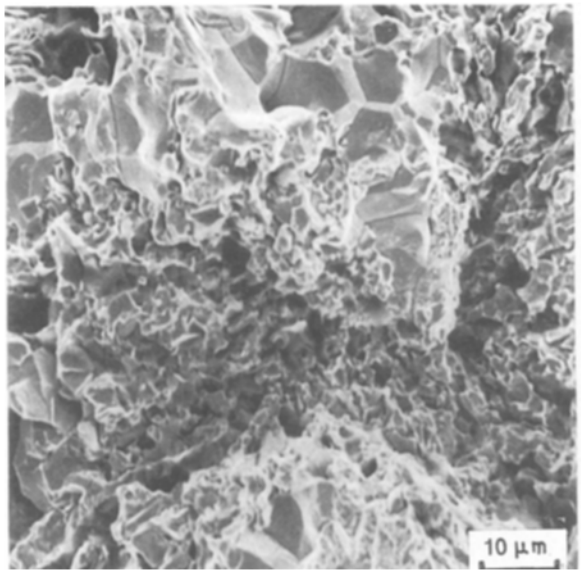

Figure 11 Scanning electron micrograph of fracture surface of sample A showing clusters of microporosity at regions of the phosphide eutectic.

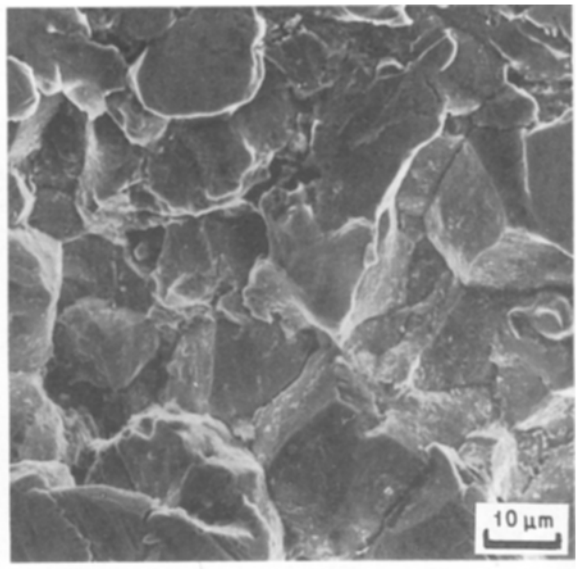

Figure 13 Scanning electron micrograph of liner surface of sample A showing machine marks on the liner surface.

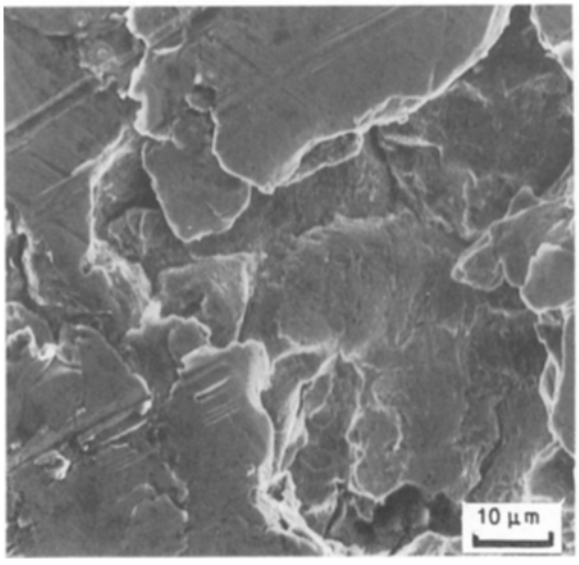

Figure 12 Scanning electron micrograph of liner surface of sample B showing metal removal during machining and marks on surface from machining operation.

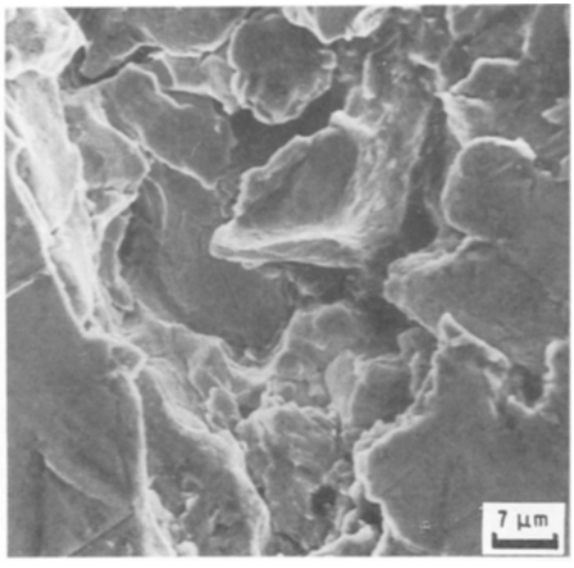

Figure 14 Scanning electron micrograph of surface pore on sample A showing cast-iron metal embedded in the surface pore.

increased porosity on the surface of sample A is rationalized as being due to the presence of an increased amount of phosphide eutectic. High magnification observation in the electron microscope was done to study the morphology of individual surface pores. At higher magnifications the regions at which the metal is torn away from areas of porosity during machining are revealed. Fine machine marks were evident on the surface (Figs 12 and 13). The jagged surface pores were found to be larger than the original regions of microporosity. The surface pores produced by machining would tend to degrade the pressure tightness of the cylinder liner, and also increase abrasive wear of the liner surface.

During machining, when the grey cast iron metal is removed from the pores, fine pieces of metal get trapped and embedded in these pores (Fig. 14). The trapped metal can be dislodged from the pore during operation of the engine and results in increased wear.

4. Concluding remarks

This study has verified that phosphorus content influences porosity. The major conclusions in using the different analytical methods are the following.

1. A higher level of phosphorus was present in the liner with 150 μm finish compared to the 40 μm sample. The higher phosphorus content resulted in higher levels of porosity, due to the formation of the phosphide eutectic.

2. High magnification SEM observations revealed metal being torn away from regions of shrinkage porosity, and fine pieces of metal were embedded in the surface pores. The fracture surface of sample A revealed the presence of large clusters of microporosity, while sample B had fewer pores that were isolated.

These results taken together suggest that while a high phosphorus content may be desirable for improved hardness, it can result in inferior wear resistance due to increased levels of porosity and trapping of wear debris in the fine pores, thus, care in processing must be emphasized when producing liners with a high phosphorus content. It would also be advisable to choose a liner composition, cooling rate and liner thickness along with minimal alloying elements if wear resistance is the key parameter of interest.

References

1. H. T. ANGUS, *Wear* **1** (1959) 40.
2. *Idem., BCIRA J.* **10** (1962) 610.
3. A. F. SPENGLER and R. A. ASHBY, *Modern Castings* **65** (1975) 520.
4. M. CLIFFORD and A. D. MORGAN, *BCIRA J.* **10** (1962) 759.
5. K. E. L. NICHOLS, *BCIRA J.* **8** (1960) 29.
6. R. D. GUNDLACH and W. G. SCHOLZ, "Phosphide Eutectic in Gray Iron Castings containing Chromium and Molybdenum," Climax Molybdenum Company, Report, 1980.
7. J. H. GITTUS and I. C. H. HUGHES, *BCIRA J.* **5** (1955) 537.
8. J. C. HAMAKER, Jr, W. P. WOOD and F. B. ROTE, *AFS Trans.* **60** (1952) 401.
9. J. M. GREENHILL, *Foundry Trade J.* **11** (1981) 787.
10. K. E. L. NICHOLS, *BCIRA J.* **10** (1962) 166.
11. H. MORROGH and P. H. TUTSCH, *J. Iron and Steel Inst.* (1954) 382.
12. H. D. MERCHANT and J. F. WALLACE, *ASF Trans.* **69** (1961) 249.
13. C. M. ADAMS, M. C. FLEMINGS and H. F. TAYLOR, *ibid.* **56** (1958) 369.

Received 2 August 1990
and accepted 12 February 1991